Co-published by
Institute of Fluid-Flow Machinery
Polish Academy of Sciences
Committee on Thermodynamics and Combustion
Polish Academy of Sciences

http://www.imp.gda.pl/archives-of-thermodynamics/

Visual and microscopic tests of composite PV module samples for the construction of roof and facade type BIPV

Piotr Sprawka[a], Patryk Chaja[b*], Paweł Wujek[a]

[a]ElectroTile Sp. z o.o., Pulawska 427, 02-801 Warszawa, Poland
[b]Institute of Fluid-Flow Machinery Polish Academy of Sciences, Fiszera 14, 80-231 Gdańsk, Poland
*Corresponding author email: patryk.chaja@imp.gda.pl

Received: 03.07.2024; revised: 30.07.2024; accepted: 09.09.2024

Abstract

The introduction of new material solutions into the BIPV (Building Integrated Photovoltaics) requires the need to check their suitability in this area. This especially applies to resistance to weather conditions and resistance to UV radiation. The authors conducted a series of tests on samples of photovoltaic modules made using a composite lamination technology based on glass fibres and hardened resins. The resistance of such a structure to atmospheric conditions and degradation by UV rays was investigated. Both of these areas have a significant impact on the efficiency of such a solution in terms of converting solar energy into electricity and the service life of the solution. It was found that delamination of the composite PV modules can be avoided in the case of some studied resins (e.g. LG 385).

Keywords: Composite; Photovoltaic; Roof; Use of lightweight structures

Vol. 45(2024), No. 4, 163–168; doi: 10.24425/ather.2024.150005

Cite this manuscript as: Sprawka, P., Chaja, P., & Wujek, P. (2024). Visual and microscopic tests of composite PV-module samples for the construction of roof and facade type BIPV. *Archives of Thermodynamics*, 45(4), 163–168.

1. Introduction

Recently, growing implementation of renewable energy sources (RES) − particularly photovoltaics, pointed to a paradigm shift in global energy systems. This transformation is largely driven by the urgent call to mitigate climate change impacts and by a rapid decline in the costs of photovoltaic technologies. Consequently, an increasing number of photovoltaic modules are being connected to power grids, a trend that is particularly noticeable in urbanized regions.

However, this exponential growth has brought to the fore a new challenge regarding the installation of a significant number of heavy photovoltaic modules on roof surfaces with specific load capacities. Notably, conventional photovoltaic installations have been found to exert substantial strain on building structures, with typical modules weighing around 12−16 kg/m² and the whole installation weighing approximately 40 kg/m² [1,2]. Such considerable weight has been identified as a limitation, especially in cases where roof structures have a lower load-bearing capacity.

To address this emerging issue, the sector has witnessed a burgeoning interest in the development of lightweight photovoltaic modules, which are commonly referred to as composite photovoltaic (CPV) modules. Such modules, presumed to weigh less than 7 kg/m² [3], present a promising avenue for expanding the integration of photovoltaic technologies, especially in urban setups with roof constraints. Besides, they eliminate the need for heavy glass and frames, components that constitute around 80% of the conventional module weight, achieving a potential weight reduction of about 2 kg/m² [4]. However, it is noteworthy that the CPV technology is distinct from building integrated photovoltaics (BIPV), which seamlessly integrates into the building's roof partitions. This distinction signifies that CPV modules offer flexibility in mounting options, allowing for the utilization of conventional mounting systems.

Nomenclature

Abbreviations and Acronyms

BIPV – building integrated photovoltaics
RES – renewable energy sources
CPV – composite photovoltaic

Despite these advancements, there remains a significant research gap in identifying optimal materials and configurations that would promote efficiency while maintaining lightweight properties. Furthermore, the sector demands meticulous scrutiny in developing coating technologies that could potentially eliminate point damages to the finished products.

This research, initiated under the auspices of the "Path for Mazovia 2019" competition, ventured into this relatively uncharted territory. Drawing upon the promising potential of composite materials, this research sought to innovate composite photovoltaic elements that not only serve as renewable energy sources elements but also function as supporting structures without the necessity of additional constructions on the roof, thereby aligning with the BIPV concept [5–7].

Much attention was paid to studies of new polymeric materials encapsulating PV (photovoltaic) elements [8]. The current state-of-the-art knowledge of different types of composites, used for the PV cell enhancement was discussed in Ref. [9], with a special focus on two-dimensional (2D) materials.

Here, the work embarked on an experimental approach wherein various resin/hardener compositions were fabricated, tested and compared including 6 types described in Refs. [10–14]. Through a series of visual and microscopic examinations, this research endeavour aims to carve out new pathways into coating technologies that satisfy manufacturer requirements while averting potential damage points in the final product.

The following characteristics of CPV samples are assessed according to the quality requirements laid down here:

- delamination surface – requirement: less than 2% of the surface, delamination in the form of stratification between the layers (compact stains) and in the form of stratification between the resin and the fabric (cross-crack mesh);
- dimension of air bubbles – requirement: less than 0.1 mm.

By weaving through these layered complexities and potential innovations, this study hopes to steer the global community a step closer to realizing a sustainable energy future with an integrated, efficient and adaptable photovoltaic solution.

2. Materials and methods

During the tests described in [10–14], 6 types of CPV samples with dimensions of 380 mm × 190 mm and of the same structure (Table 1) were produced; they differ in resins and hardeners used. Two cells measuring 156 mm × 156 mm were placed in the samples, see Fig. 1. The specification of the resins with dedicated hardeners is shown in Table 2. The samples were described by the composition of the resin/hardener as shown in Table 3. Visual and microscopic examinations were carried out on 3 samples in the initial state and 9 samples after accelerated aging in the climatic chamber.

Tests in the thermoclimatic chamber were carried out in accordance with the IEC 61215:2005 standard (Fig. 2). The purpose of this test was to determine the resistance of the photovoltaic module to the effects (material fatigue, temperature stress, etc.) of rapid temperature changes from 85°C down to –40°C. These tests stress the photovoltaic module, as a result of which, the different thermal expansion coefficients of the photovoltaic module parts reveal hidden defects such as poor soldering, cracked cells, delamination, efficiency reduction and insulation resistance, etc.).

Table 1. Structure of CPV samples for quality testing.

Layer subgroup	Layer number	Layer marking	Fibre direction	Total thickness
Top layers	7	Resin	0/90	2.1 mm
	6	GFRP TKAN. 163	–	
Cell	5	2 layers of EVA* film	–	
	4	2 layers of EVA film	–	
	3	2 layers of EVA film	–	
Bottom layers	2	Resin and black pigment	–	
	1	GFRP TKAN. 390	0/90	

*EVA – ethylene vinyl acetate.

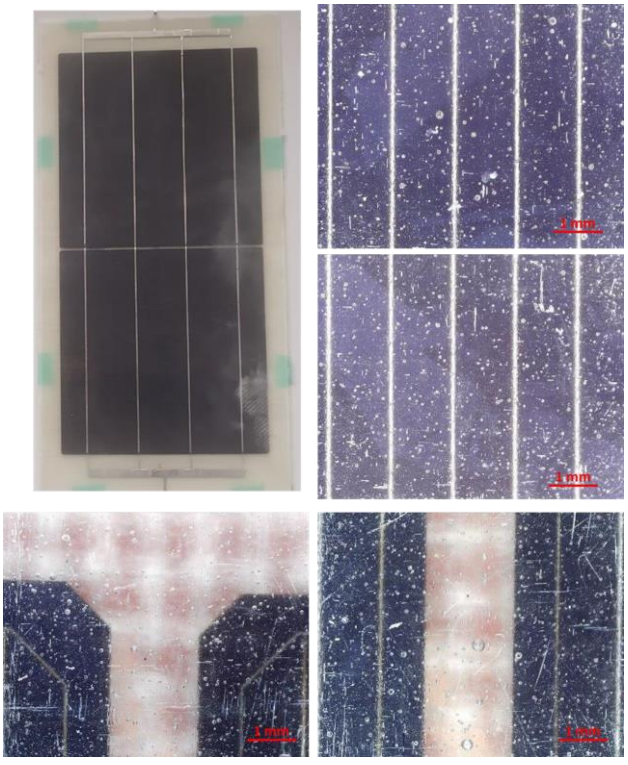

Fig. 1. Outer surface of the sample LG 385_HG 512_1.

3. Results and discussion

The results of the visual and microscopic examinations of the samples are described in Table 4 and selected examples are shown in Figs. 1 and 3. Technological and operating defects resulting from accelerated aging in the climatic chamber were observed.

Table 2. Experimental conditions.

No.	Resin	Hardener	Resin/ hardener proportion	Heating time (h)	Heating temperature (°C)
1	LG 285	H 512	100 : 40	2	120
2	LG 285	HG 287	100 : 40	2	120
3	LG 120	HG 356	100 : 35	2	120
4	LG 900UV	HG 120	100 : 25	6	115
5	LG 385	H 512	100 : 23	2	120
6	LG 385	HG 387	100 : 40	2	120

Table 3. CPV samples descriptions.

Serial no.	Sample determination CPV	Condition
1	LG 285_H 512_1	after aging
2	LG 285_HG 287_1	after aging
3	LG 120_HG 356_1	after aging
4	LG 900UV_HG 120_1	after aging
5	LG 385_H 512_1	after aging
6	LG 385_HG 387_1	initial
7	LG 285_H 512_2	after aging
8	LG 285_HG 287_2	initial
9	LG 120_HG 356_2	after aging
10	LG 900VV_HG 120_2	after aging
11	LG 385_H 512_2	after aging
12	LG 385_HG 387_2	initial

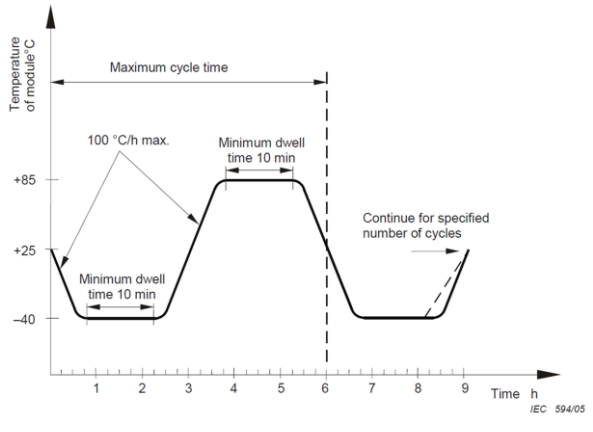

Fig. 2. Outer surface of the sample LG 385_HG 512_1.

Technical faults:

- small air bubbles of diameter less than 0.1 mm on all analysed samples (Figs. 1 and 3);
- air bubbles with dimensions from 0.2 mm to 0.5 mm on test samples: LG 285_HG 287_1, LG 120_HG 356_1, LG 900VV_HG 120_1, LG 285_HG 512_2, LG 285_HG 287_2, LG 120_HG 356_2 (Fig. 3), LG 385_HG 512_2.

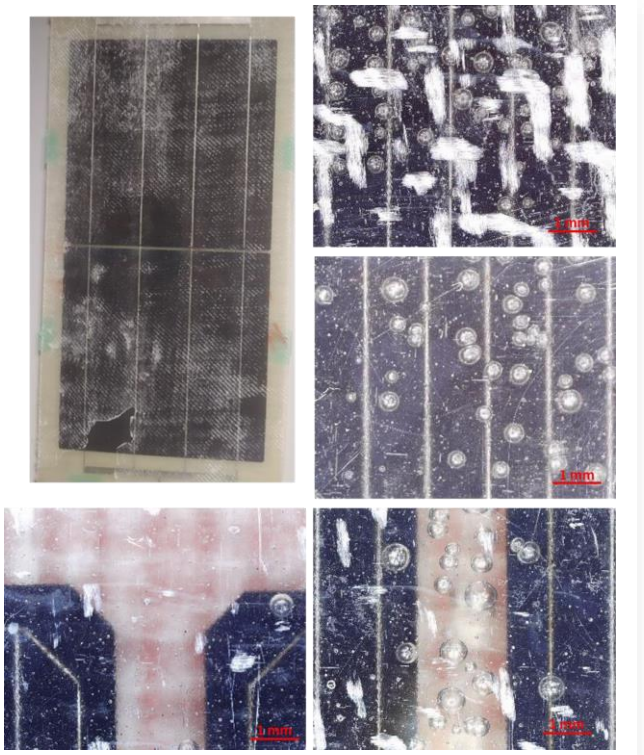

Fig. 3. Outer surface of the sample LG 120_HG 356_2 after aging.

Operating faults (after ageing):

- white structure of delamination between glass fabric and resin seen on samples: LG 285_HG 287_1, LG 120_HG 356_1, LG 285_HG 512_2, LG 900UV_HG 120_2, LG 385_HG 512_2 (see left top in Fig. 3);
- white dots on the sample LG 120_HG 356_2 (see bottom of Fig. 3);
- extensive white fields covering most of the surface of the top layer resulting from the degradation of the resin during aging (see right top in Fig. 3).

Efficiency testing of the manufactured composite modules indicates that small air inclusions with a diameter below 0.1 mm are acceptable. Larger inclusions cause delamination and ultimately degradation and rapid destruction of the module. Air inclusions have also a strong impact on the mechanical strength of the composite, causing the formation and propagation of micro-cracks. This leads to mechanical damage to the CPV module. Table 5 summarizes the characteristics examined and compares them with the required quality criteria.

Performed studies have shown that defects in the form of delamination are formed only after the aging process – see Figs. 1 and 3. No delamination was observed in the initial samples immediately after the production process. In most test samples, delamination after aging takes various forms, such as

Table 4. The results of visual and microscopic examinations of CPV samples.

Sample	Examined feature	Description	Sample condition	Sample	Examined feature	Description	Sample condition
LG 285_H 512_1	Delamination	Extensive whiteness covering most of the outer surface of the upper layer. White cross-mesh indications of trace delamination between the fabric and the top layer resin covering most of the surface of the top layer.	After aging	LG 285_H 512_2	Delamination	Extensive whiteness covering most of the outer surface of the upper layer. White cross-mesh indications of trace delamination between the fabric and the top layer resin covering most of the surface of the top layer.	After aging
	Air bubbles	Small air bubbles of less than 0.1 mm.			Air bubbles	Small air bubbles of less than 0.1 mm in size. Air bubbles with a dimension between 0.2 and 0.5 mm in size located in.	
	Other	Colouring resin in yellow.			Other	Colouring resin in yellow.	
LG 285_HG 287_1	Delamination	White cross-mesh indications of trace delamination between the fabric and the top layer resin covering most of the surface of the top layer.	After aging	LG 285_HG 287_2	Delamination	Absence	Initial
	Air bubbles	Small air bubbles with a dimension of less than 0.1 mm. Air bubbles with a dimension between 0.2 and 0.5 mm.			Air bubbles	Small air bubbles with a dimension of less than 0.1 mm. Air bubbles with a dimension between 0.2 and 0.5 mm	
	Other	Colouring resin in yellow.			Other	Colouring resin in green.	
LG 120_HG 356_1	Delamination	White cross-mesh indications of trace delamination between the fabric and the top layer resin.	After aging	LG 120_HG 356_2 (Fig. 2)	Delamination	White indications of trace delamination at short sections of the upper edge of the glass fabric, located on a significant surface of the top layer.	After aging
	Air bubbles	Small air bubbles with a dimension of less than 0.1 mm. Air bubbles with a dimension between 0.2 and 0.5 mm, located in small areas of the top layer.			Air bubbles	Small air bubbles of less than 0.1 mm.	
	Other	Colouring resin in yellow.			Other	Colouring resin in yellow. Flaking on the outer surface.	
LG 900VV_HG 120_1	Delamination	Absence	After aging	LG 900VV_HG 120_2	Delamination	White indications of trace delamination at short sections of the upper edge of the glass fabric, located on a significant surface of the top layer.	After aging
	Air bubbles	Small air bubbles with a dimension of less than 0.1 mm. Air bubbles with a dimension between 0.2 and 0.5 mm, located in small areas of the top layer.			Air bubbles	Small air bubbles with a dimension of less than 0.1 mm. Air bubbles with a dimension between 0.2 and 0.5 mm.	
	Other	Colouring resin in yellow.			Other	Colouring resin in yellow.	
LG 385_H 512_1 (Fig. 1)	Delamination	Absence	After aging	LG 385_H 512_2	Delamination	White cross-mesh indications of trace delamination between the fabric and the top layer resin covering most of the surface of the top layer.	After aging
	Air bubbles	Small air bubbles of less than 0.1 mm.			Air bubbles	Small air bubbles with a dimension of less than 0.1 mm. Air bubbles with a dimension between 0.2 and 0.5 mm.	
	Other	Colouring resin in yellow.			Other	Colouring resin in yellow.	
LLG 385_HG 387_1	Delamination	Absence	Initial	LLG 385_HG 387_2	Delamination	Short cracks in one direction along the fibre of the glass fabric, which are a trace of delamination of the individual fibres of the outer fabric of the glass, covering most of the outer surface.	Initial
	Air bubbles	Small air bubbles of less than 0.1 mm.			Air bubbles	Small air bubbles of less than 0.1 mm.	
	Other	Colouring resin in green.			Other	Colouring resin in green.	

Table 5. Characteristics of the tested CPV samples – fulfilment of the design requirements.

Sample	Examined feature	Measured value	Limit value	Is condition met?
LG 285_H 512_1	Delamination	~ 60%	< 2% total surface	NO
	Air bubbles	up to 0.5 mm	< 0.1 mm	NO
LG 285_HG 287_1	Delamination	~ 50%	< 2% total surface	NO
	Air bubbles	up to 0.5 mm	< 0.1 mm	NO
LG 120_HG 356_1	Delamination	~ 60%	< 2% total surface	NO
	Air bubbles	up to 0.5 mm	< 0.1 mm	NO
LG 900UV_ HG 120_1	Delamination	< 2%	< 2% total surface	YES
	Air bubbles	up to 0.5 mm	< 0.1 mm	NO
LG 385_H 512_1 (Fig. 1)	Delamination	< 2%	< 2% total surface	YES
	Air bubbles	< 0.1 mm	< 0.1 mm	YES
LG 385_HG 387_1	Delamination	< 2%	< 2% total surface	YES
	Air bubbles	< 0.1 mm	< 0.1 mm	YES
LG 285_H 512_2	Delamination	~ 70%	< 2% total surface	NO
	Air bubbles	up to 0.5 mm	< 0.1 mm	NO
LG 285_HG 287_2	Delamination	< 2%	< 2% total surface	YES
	Air bubbles	up to 0.5 mm	< 0.1 mm	NO
LG 120_HG 356_2 (Fig. 2)	Delamination	~ 100%	< 2% total surface	NO
	Air bubbles	up to 0.5 mm	< 0.1 mm	NO
LG 900VV_ HG 120_2	Delamination	~60%	< 2%total surface	NO
	Air bubbles	< 0.1 mm	< 0.1 mm	YES
LG 385_H 512_2	Delamination	~ 60%	< 2%total surface	NO
	Air bubbles	< 0.1 mm	< 0.1 mm	YES
LLG 385_ HG 387_2	Delamination	~ 60%	< 2% total surface	NO
	Air bubbles	< 0.1 mm	< 0.1 mm	YES

dense bleaching (delamination between layers) and gradual fading. This ultimately leads to damage to the element at a level that prevents its further use.

Studies have shown that the size of the air bubbles can be divided into two ranges: 1) below 0.1 mm (evenly distributed over the surface of the sample): and 2) from 0.2 to 0.5 mm (locally distributed).

Two test samples based on LG 385 resin (LG 385_H 512_1 and LG 385_HG 387_1) met the quality requirements both in terms of the allowable delamination surface and the allowable size of air bubbles. These criteria are also met by samples based on crystalline resin, which were used in other tests as part of the first stage of the investigations.

Samples that meet the requirements have inclusions, but their number and size do not affect the efficiency and durability of the PV module.

The following conclusions can be drawn from the studies:

- Air bubbles above 0.1 mm in size can be prevented or significantly reduced when the established technological regime is kept during production.
- The selection of the appropriate resin and hardener as well as the appropriate preparation of PV panels will reduce the formation of delamination during operation.

Moving forward, the results from the current study propose a promising solution for further research. Here, we have identified that adherence to established technological regimes can effectively reduce or even eliminate the formation of air bubbles that exceed 0.1 mm. This insight necessitates a detailed exploration into optimizing the technological regimes to further enhance the efficiency and longevity of CPV modules. Moreover, a meticulous selection and preparation of resins, hardeners and PV panels could substantially mitigate the formation of delaminations during operation, indicating a vital area where future research could be channelized.

Furthermore, future research should aim at:

- developing a deeper understanding of the aging process and its influence on delamination, possibly steering towards the innovation of aging-resistant materials and technologies;
- exploring new composite materials that potentially could offer better resilience against the formation of air inclusions and delaminations;
- designing real-time monitoring systems to detect and address defects at early stages, preventing rapid degradation and promoting the longevity of the modules;
- collaborating with industry to facilitate the transition from research to real-world applications, ensuring that the advancements made in the labs can significantly impact the global movement towards sustainable energy.

The study presents a significant step towards optimizing the production and efficiency of composite photovoltaic modules. By leveraging the insights gained from this research, there exists a potential pathway to revolutionize the renewable energy sector with lightweight, efficient and durable photovoltaic solutions. As we forge ahead, continuous exploration and innovation in material science and technology regimes stand pivotal in steering the global community towards a sustainable energy future.

6. Conclusions

Qualitative research of aging of PV modules indicated that defects in the form of delamination arise only after the aging process. Delamination was not observed in the baseline samples, immediately after the manufacturing process. Delamination after aging in most test samples takes various forms such as compact bleaching (stratification between layers) and bleaching in the form.

Studies have shown that the size of air bubbles can be divided into two ranges: 1) below 0.1 mm (evenly distributed over the sample surface) and 2) from 0.2 to 05 mm (locally distributed). Air bubbles above 0.1 mm can be reduced or removed

completely as a result of strict compliance with the established technological regime.

Choosing the right resin and hardener and proper preparation of the PV panels will allow us to reduce the formation of delamination during operation. Two LG 385 resin-based test samples met the quality requirements both in terms of the permissible delamination surface and the acceptable size of air bubbles. These criteria are also met by samples based on crystalline resin which were tested in previous studies.

Further work related to BIPV is planned as part of the cooperation between ElectroTile Sp. z o.o. and IMP PAN/KEZO Research Centre. A newly conducted research project focuses on the implementation of new PV products into series production.

Acknowledgements

This work was carried out as part of the implementation of the research project entitled: "Building Sun System – photovoltaic composite roofing and facade system: BIPV II generation", MAZOWSZE/0134/19 and was also supported by the Polish Ministry of Science and Higher Education in the frame of Implementation Doctorate Programme (II edition) – Agreement No. 0063/DW/2018 from 2 August 2018.

References

[1] Ferroni, F., & Hopkirk, R.J. (2016). Energy Return on Energy Invested (ERoEI) for photovoltaic solar systems in regions of moderate insolation. *Energy Policy*, 94, 336–344. doi: 10.1016/j.enpol.2016.03.034.

[2] Mik, K., Zawadzki, P., Tarłowski, J., & Bykuć S. (2022). Assessment of prototype lightweight photovoltaic modules after over 1-year field test in Polish conditions. *Renewable Energy*, 198, 1008–1020. doi: 10.1016/j.renene.2022.08.104

[3] Martins, A.C., Chapuis, V., Virtuani, A., Perret-Aebi, L.-E., & Ballif, C. (2017). Hail resistance of composite-based glass-free lightweight modules for building integrated photovoltaics applications. *33rd European Photovoltaic Solar Energy Conference and Exhibition*, 25–29 September 2017, Amsterdam, Netherlands. doi: 10.4229/EUPVSEC20172017-6BV.3.62

[4] Oreski, G., Stein, J.S., Eder, G.C., Berger, K.A., Bruckman, L.S., Vedde, J., Weiß, K., Tanahashi, T., French, R.H., & Ranta, S. (2021). *Designing new materials for photovoltaics: Opportunities for lowering cost and increasing performance through advanced material innovations*. Report IEA-PVPS T13-13:2021. doi: 10.2172/1779380

[5] Berger, K., Cueli, A.B., Boddaert, S., Buono, M.D., Delisle, V., Fedorova, A.S., Frontini, F., Hendrick, P., Inoue, S., Ishii, H., Kapsis, C., Kim, J., Kovács, P., Chivelet, N.M., Maturi, L., Machado, M., Schneider, A., & Wilson, H.R. (2018). *International definitions of "BIPV"*. Report IEA-PVPS T15-04: 2018: doi: 10.13140/RG.2.2.15351.68007

[6] Ghosh, A (2020). Potential of building integrated and attached/applied photovoltaic (BIPV/BAPV) for adaptive less energy-hungry building's skin: A comprehensive review. *Journal of Cleaner Production*, 276, 123343. doi: 10.1016/j.jclepro.2020.123343

[7] Martins, A.C., Chapuis, V., Sculati-Meillaud, F., Virtuani, A., & Ballif, C (2018). Light and durable: Composite structures for building-integrated photovoltaic modules. *Progress in Photovoltaic Research and Applications.* 26(9), 718–729. doi: 10.1002/pip.3009

[8] Gaddam, S.K., Pothu, R., & Rajender Boddula, R. (2021). Advanced polymer encapsulates for photovoltaic devices − A review. *Journal of Materiomics*, 7, 920–928. doi: 10.1016/j.jmat.2021.04.004.

[9] Olorunfemi, T.R., Nwulu, N.I., & Ismail, S.O. (2022). Composites as candidate materials for photovoltaic cells. *Advances in Materials and Processing Technologies*, 8(4), 2378–2397. doi: 10.1080/2374068X.2022.2046328

[10] Kajisa, T., Miyauchi, H., Mizuhara, K., Hayashi, K., Tokimitsu, T., Inoue, M., Hara, K., & Masuda, A. (2014). Novel lighter weight crystalline silicon photovoltaic module using acrylic-film as a cover sheet. *Japanese Journal of Applied Physics*, 53, 092302. doi: 10.7567/JJAP.53.092302

[11] Mik, K., Bugaj, M., & Chaja, P. (2021). The evaluation of the snail track affected photovoltaic modules by different methods after 3-year operating in central Poland. *Renewable Energy*, 163, 504–516. doi: 10.1016/j.renene.2020.09.005

[12] Nussbaumer, H., Klenk, M., & Keller, N. (2016). Small unit compound modules: a new approach for light weight PV modules. 32rd European Photovoltaic Solar Energy Conference and Exhibition, 20–24 June 2016, Munich, Germany. doi: 10.4229/EUPVSEC20162016-1BO.12.5

[13] Schindler, S., Götz, D., & Dassler, D. (2019). Lightweight PV module approach − field test study and yield evaluation. *36th European Photovoltaic Solar Energy Conference and Exhibition*, 9–13 September 2019, Marseille, France. doi: 10.4229/EUPVSEC20192019-1BO.9.5.

[14] Martins, A.C., Chapuis, V., Virtuani, A., & Ballif, C. (2019). Robust glass-free lightweight photovoltaic modules with improved resistance to mechanical loads and impact. *IEEE Journal of Photovoltaics*, 9(1), 245–251. doi: 10.1109/JPHOTOV.2018.2876934